



ISSN 2790 – 5985

e ISSN 2790 – 5993

Agriculture College – Wasit University

Dijlah J. Agric. Sci., 2(2):141-148, 2024

Dijlah Journal of  
Agricultural Sciences

## Identification of Potential Inhibitors for *Fasciola hepatica* Glutathione Transferase Using Molecular Docking and Virtual Screening

Mrtatha K. Al - Zrkani

Department of Animal Production, College of Agriculture, Wasit University

\*Corresponding author e-mail: [malzrkani@uowasit.edu.iq](mailto:malzrkani@uowasit.edu.iq)

### Abstract:

*Fasciola hepatica*, the parasitic flatworm responsible for fascioliasis, a serious neglected tropical disease, remains a serious threat to human and animal health worldwide. The parasite's glutathione transferase (GST) enzyme plays a crucial role in detoxifying xenobiotics and endogenous compounds and is therefore a desirable target for drug action.

This study used molecular docking and virtual screening approaches to screen for potential small-molecule inhibitors of *F. hepatica* GST, the aim of finding novel anti-fascioliasis drug leads. 100 compounds were screened from the ZINC database for FDA-approved drugs. Molecular docking simulations were performed to determine the binding affinities of the ligands for the GST active site, where a number of potential candidates emerged. The highly ranked ligands showed high binding affinities with primary interactions in the form of hydrogen bonding, electrostatic interactions, and hydrophobic forces. Among these, the highest binding energy of -8.4 kcal/mol was associated with (ZINC000026664090), revealing its lead status for potential development into a new drug. Such findings provide crucial information on how to design efficacious inhibitors against *F. hepatica* GST and represent a bright direction for future development of fascioliasis therapeutics.

**Keywords:** Molecular Docking, *Fasciola hepatica*

تحديد المثبطات المحتملة لإنزيم الجلوتاثيون ترانسفيراز في *Fasciola hepatica* باستخدام الإرساء الجزيئي والفحص الافتراضي

مرتضى كريم علي

قسم الانتاج الحيواني/ كلية الزراعة/ جامعة واسط

الخلاصة

*Fasciola hepatica*، الدودة المسطحة الطفيلية المسؤولة عن fascioliasis، وهو مرض استوائي مهم وخطير، لا يزال يشكل تهديدًا كبيرًا لصحة الإنسان والحيوان في جميع أنحاء العالم. يلعب إنزيم الجلوتاثيون ترانسفيراز (GST) للطفيل دورًا حاسمًا في إزالة سموم المركبات الغريبة والمركبات الداخلية، وبالتالي فهو هدف مرغوب فيه لتطوير الأدوية. استخدمت هذه الدراسة تقنيات

الالتحام الجزيئي والفحص الافتراضي لفحص مثبطات محتملة من الجزيئات الصغيرة لـ *F. hepatica* GST ، بهدف العثور على مرشحات جديدة لأدوية مضادة للفاسيوليا. تم فحص 100 مركب من قاعدة بيانات ZINC الخاصة بالأدوية المعتمدة من إدارة الغذاء والدواء الأمريكية. تم إجراء محاكاة الالتحام الجزيئي لتحديد affinities التفاعل للجزيئات في موقع الإنزيم النشط لـ GST ، حيث ظهرت عدة مرشحات محتملة. أظهرت الجزيئات الأعلى تصنيفاً affinity عالية مع التفاعلات الرئيسية في شكل الروابط الهيدروجينية، والتفاعلات الكهروستاتيكية، والقوى الكارهة للماء. من بين هذه المركبات، كانت أعلى طاقة ارتباط 8.4 كيلو كالوري/مول مرتبطة بـ ZINC000026664090 ، مما يكشف عن وضعه كمرشح رئيسي للتطوير المحتمل إلى دواء جديد. تقدم هذه النتائج معلومات حاسمة حول كيفية تصميم مثبطات فعالة ضد *F. hepatica* GST وتمثل اتجاهاً مشرفاً لتطوير العلاجات المستقبلية fascioliasis.

الكلمات المفتاحية: *Fasciola hepatica* ، الإرساء الجزيئي، إنزيم (GST).

## Introduction

*Fasciola hepatica*, a parasitic flatworm, is the causative agent of fascioliasis, a neglected tropical disease affecting both humans and livestock worldwide. The parasite's glutathione transferase enzyme has been identified as a potential drug target due to its crucial role in the detoxification of xenobiotics and endogenous compounds (Lalor et al., 2021). In this study, we employ molecular docking and virtual screening approaches to identify potential small-molecule inhibitors of *F. hepatica* glutathione transferase that could serve as lead compounds for the development of novel anti-fascioliasis drugs .

*Fasciola hepatica*, along with its counterpart *Fasciola gigantica*, is a highly prevalent species of liver fluke that drives the zoonotic disease fasciolosis in both livestock and human populations globally (Hu et al., 2022; Li & Liu, 2024). This trematode parasite primarily instigates food-borne fasciolosis, affecting domestic ruminants in tropical and temperate regions as well as an expanding range of wild animal hosts. Although traditionally viewed as a livestock ailment, fasciolosis has emerged as a significant public health concern, with millions of humans now at risk of infection worldwide. The adult *F. hepatica* flukes, measuring 20-40 mm in length and 8-13 mm in width, are flatworms that pose a serious threat to the wellbeing of animals and humans alike (Lalor et al., 2021; Nawar et al., 2024).

Globally, the total number of human fasciolosis cases is estimated to be 2.4 –17 million, with 180 million people at risk of infection (Zhou et al., 2019).

The current treatment for fasciolosis relies on a limited number of drugs, primarily triclabendazole and albendazole, which have shown increased resistance in some regions. Therefore, the development of new therapeutic options is crucial to combat this disease .

Glutathione transferases are a family of multifunctional enzymes that play a vital role in the detoxification of xenobiotics and endogenous compounds in *F. hepatica* (Su et al., 2024). These enzymes catalyze the conjugation of glutathione to various electrophilic substrates, rendering them less toxic and more easily excreted. Targeting the *F. hepatica* glutathione transferase enzyme could be a promising strategy for the development of novel anti-fascioliasis drugs (Allocati et al., 2018; Shoulah et al., 2024).

In this study, we aim to identify potential small-molecule inhibitors of *Fasciola hepatica* glutathione transferase using the ZINC database through a combination of molecular docking and virtual screening approaches.

## 2. Material and Method

### 2.1 Protein selection and preparation

The MIP-dimensional structure was retrieved from RCSB Protein Data Bank (PDB ID: 8BJE). Protein structure resolution 1.50 Å. water molecules in the protein structure were removed using Pymol software (Chen et al., 2021). Using the AutoDockVina software (Trott & Olson, 2010), polar hydrogen atoms were added, followed by Kollman and Gasteiger charges were added to the amino acid residues of the protein structure

### 2.2. Ligand structure preparation

The 2 D ligand coordinates were retrieved from the ZINC database FDA Approved drugs, per Drug Bank (<https://zinc.docking.org/substances/subsets/fda/>). Open Babel 3.1.1 software were used for ligand preparation (Al-Zrkani et al., 2023), all the ligands were converted to a 3D sdf file.

### 2.3. Molecular Docking

AutoDock Vina was used for the molecular docking of the candidate, considering the confined co-crystalline binding site as a chemical search space (Dallakyan & Olson, 2015). The Lamarckian genetic method created the score function for ligands docked inside the Grid Box. AutoDockVina was used in this study for molecular docking. Grid Box was generated using GSH co-ligand active site residues TRP7, TRP40, ASN53, ASN53, and TYR110 with coordinates of **X: 98.75, Y: 95.55, Z: -48.40** (Å) to select interaction area of monomers.

## Result and Discussion

### Molecular Docking

In the present study, in silico docking simulation screened 100 compounds from a public database to unveil potential Glutathione Transferase (GST) inhibitors. Molecular docking was conducted by Autodock, used for virtual screening ligands from the zinc database against the GSH co-ligand active site of 1FHE (FH47) from fasciola hepatica. Autodock scores were used to rank the docking output and the ligands that show lower docking scores showing (Table 1).

Table 1: Affinity of autodocking vina.

ID	Affinity(kcal/mol)	Hydrogen Bonding Interactions
GSH	-5	TRP7, TRP40, ASN53, ASN53, TYR110
ZINC000026664090	-8.4	TYR6, TYR6, TRP7, ASN53, ASN53
ZINC000019632917	-7	TYR6
ZINC000060392785	-7	TYR6, TRP7, TRP40, LYS44:H22, LYS44
ZINC000003830958	-6.6	TYR6, TRP7, ARG37, ASN203, TYR110, GLN66, SER67

### Molecular Docking Analysis of Selected Ligands with Target Protein

Molecular docking simulations were performed to evaluate the binding interactions of five ligands co-ligand, ZINC000026664090, ZINC000019632917, ZINC000060392785, and ZINC000003830958 within the active site of the target protein. The analysis revealed notable differences in binding affinities and interaction patterns, including hydrogen bonding, electrostatic interactions, and hydrophobic forces, which collectively contribute to ligand stability and binding efficiency showing in (Figure 1).

Co-ligand exhibited a moderate binding affinity of -5 kcal/mol, primarily stabilized by electrostatic interactions, hydrogen bonds, and hydrophobic contacts. Strong salt bridges were observed with ARG37 (HH21, 2.74 Å) and LYS44 (HZ3, 1.99 Å), suggesting a key role of electrostatic interactions in stabilizing the ligand. Additional attractive charge interactions with ARG37 (NH2, 5.11 Å), LYS44 (NZ, 4.74 Å), and ARG102 (NH2, 3.91 & 4.42 Å) reinforced ligand orientation in the active site. Hydrogen bonding further contributed to stability, with TYR110: OH (1.69 Å) forming the strongest interaction, followed by TRP7:HE1 (1.93 Å), TRP40:HE1 (2.01 Å), and ASN53:OD1 (2.48 & 2.52 Å). Carbon hydrogen bonds with GLY11:HA2 (2.48 Å) and GLY106:HA3 (2.98 Å) provided additional support for ligand retention in the binding pocket.

(ZINC000026664090) exhibited the strongest binding affinity (-8 kcal/mol), indicating highly stable ligand-protein interactions. Hydrogen bonding played a dominant role, with TRP7:HE1 (1.80 Å) forming the strongest hydrogen bond, followed by interactions with TYR6: HH (2.48 & 2.95 Å) and ASN53:OD1 (2.02 & 2.55 Å). A  $\pi$ -donor hydrogen bond was also observed with ASN53:HD22 (3.11 Å), suggesting additional stabilization through  $\pi$ -electron contributions. Hydrophobic interactions further enhanced binding affinity, particularly  $\pi$ - $\pi$  stacking with TRP7 (5.60 Å) and alkyl interactions with LEU12 (4.41 & 4.07 Å), ARG102 (3.67 Å), and CYS109 (4.59 Å). Additionally,  $\pi$ -alkyl interactions with TYR110 (4.63 Å) and ALA206 (5.11 Å) further reinforced ligand compatibility within the active site, supporting its superior binding strength.

(ZINC000019632917) displayed a strong binding affinity of -7.4 kcal/mol, with stabilization primarily driven by hydrogen bonding and hydrophobic interactions. The most significant hydrogen bond was observed with TYR6: HH (1.67 Å), indicating a highly stable interaction. Further hydrogen bonding with TYR110: OH (2.25 Å) contributed to additional ligand stabilization. Hydrophobic interactions, particularly  $\pi$ - $\pi$  stacking with TYR110 (4.08 Å), played a crucial role in enhancing ligand retention in the binding pocket. Moreover,  $\pi$ -alkyl interactions with TYR110 (4.64 Å) provided additional non-covalent stabilization, reinforcing the ligand's strong binding affinity.

(ZINC000060392785) demonstrated a binding affinity of -7.1 kcal/mol, with electrostatic and hydrogen bonding interactions as the primary stabilizing forces. Salt bridges and attractive charge interactions with ARG37 (HH12, HH22, HH21) and LYS44 (HZ1, HZ3, NZ), with distances ranging from 1.72 to 3.29 Å, contributed to strong electrostatic stabilization. Hydrogen bonding was also a major factor, with significant interactions observed with TYR6: HH (1.77 Å), TRP7:HE1 (2.48 Å), TRP40:HE1 (1.82 Å), LYS44:HZ2 (1.88 Å), and LYS44:HZ3 (1.92 Å), all within favorable binding distances. Carbon hydrogen bonds with ASN53:OD1 (2.20–2.85 Å) and LEU54:O (2.49–2.91 Å) provided moderate stabilizing effects. Hydrophobic interactions were limited, with a single  $\pi$ -alkyl interaction with TYR110 (4.85 Å), contributing to ligand retention within the binding site.

(ZINC000003830958) exhibited a binding affinity of -6.7 kcal/mol, with ligand stability largely dictated by hydrogen bonding and hydrophobic interactions. Among the strongest hydrogen bonds were those with SER67: OG (1.989 Å), TYR110: OH (2.006 Å), GLN66:OE1 (2.035 Å), TRP7:HE1 (2.063 Å), and TYR6: HH (2.080 Å). Additional hydrogen bonding interactions within a moderate range (2.5–3.0 Å) were observed with ARG37:HH21 (2.657 Å), ASN203:HD21 (2.603 Å), and ARG102:O (2.607 & 2.721 Å), contributing to ligand retention in the binding site. Carbon hydrogen

bonds, while weaker, further supported ligand stability, involving ARG102:O (2.607 & 2.721 Å), TYR110: OH (2.417 Å), LEU54:O (2.593 Å), and ASN53:OD1 (3.002 Å). Hydrophobic interactions were also present, with alkyl interactions involving ILE103 (4.48 Å) and  $\pi$ -alkyl interactions with LEU12 (4.45 Å), reinforcing the ligand's binding affinity.

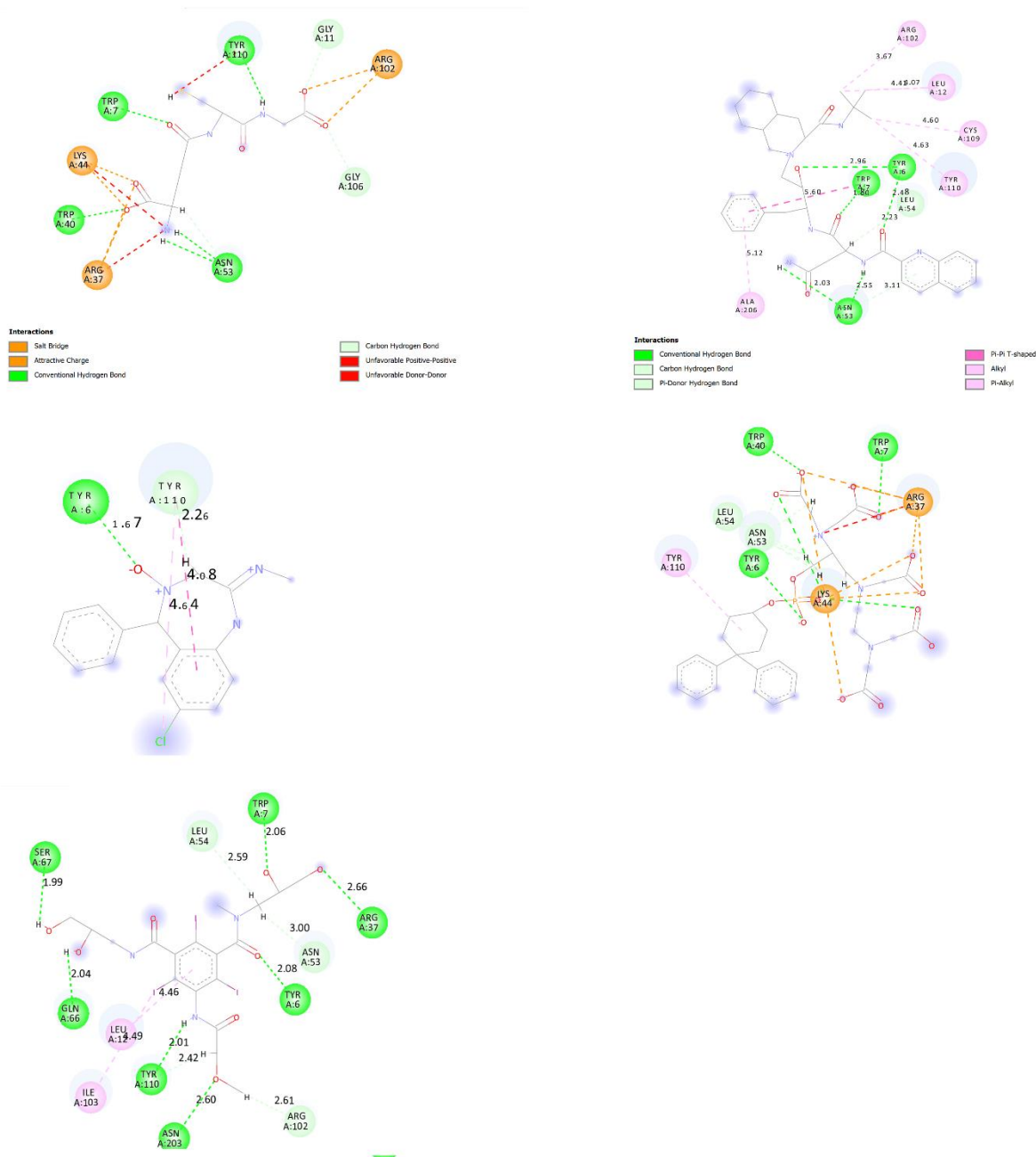


Figure 1: 2D of protein ligand interaction.

The results of the molecular docking simulations presented here offer valuable insights into the interactions between the five ligands—Co-ligand, ZINC000026664090, ZINC000019632917, ZINC000060392785, and ZINC000003830958—and the target protein. These interactions were characterized by varying binding affinities, which were influenced by multiple factors, including hydrogen bonding, electrostatic interactions, and hydrophobic forces. This comprehensive

understanding of ligand-protein interactions is crucial for the design of potent inhibitors and for advancing therapeutic applications in drug development.

Among the ligands tested, ZINC000026664090 emerged as the most promising candidate, with the highest binding affinity of -8 kcal/mol. This high affinity is primarily attributed to the strong hydrogen bonding between TRP7:HE1 (1.80 Å) and ZINC000026664090, alongside extensive hydrophobic interactions, including  $\pi$ - $\pi$  stacking with TRP7 at a distance of 5.60 Å. Hydrogen bonds and  $\pi$ - $\pi$  stacking are known to play crucial roles in stabilizing ligand-protein interactions, particularly in enhancing specificity and binding strength (Andrianov et al., 2022). The hydrophobic interactions in ZINC000026664090, which help anchor the ligand in the binding pocket, further contribute to its high binding affinity. This combination of strong hydrogen bonds and hydrophobic forces makes ZINC000026664090 an ideal candidate for further optimization as a lead inhibitor.

ZINC000019632917 demonstrated a binding affinity of -7.4 kcal/mol, stabilizing the interaction primarily through a strong hydrogen bond with TYR6: HH (1.67 Å) and  $\pi$ - $\pi$  stacking with TYR110 (4.08 Å). These interactions suggest that aromatic residues in the target protein play an important role in ligand stabilization, which has been observed in other studies focusing on  $\pi$ - $\pi$  stacking interactions (Zhang et al., 2024). The slightly lower binding affinity of ZINC000019632917 compared to ZINC000026664090 suggests that while the ligand's hydrogen bonding and hydrophobic interactions are significant, they may be less extensive or less favorable in comparison to ZINC000026664090. However, its strong interaction with aromatic residues presents an opportunity for further optimization to improve binding affinity.

ZINC000060392785, with a binding affinity of -7.1 kcal/mol, relied on electrostatic interactions such as salt bridges between ARG37 and LYS44, as well as hydrogen bonds with TYR6 and TRP7. Electrostatic interactions, including salt bridges, are well known to contribute to the stability of ligand-protein complexes by providing complementary charge-based interactions (Bissantz et al., 2010). The presence of both electrostatic and hydrogen bonding interactions in ZINC000060392785 underscores the multifaceted nature of ligand binding, indicating that further optimization of these interactions could potentially improve its binding efficiency.

ZINC000003830958, with a binding affinity of -6.7 kcal/mol, displayed multiple hydrogen bonding interactions (e.g., SER67: OG at 1.989 Å, TYR110: OH at 2.006 Å) and hydrophobic contacts. Despite these favorable interactions, its relatively lower binding affinity suggests that the ligand may benefit from further optimization, especially in terms of increasing the number or strength of its hydrophobic interactions. The combined presence of hydrogen bonds and hydrophobic interactions, however, still highlights the potential of ZINC000003830958 as a moderate binder.

The control ligand, Co-ligand, showed the lowest binding affinity (-5 kcal/mol) with moderate hydrogen bonding and electrostatic interactions. While it demonstrated some potential, its weaker affinity suggests that it may require further modification to enhance its efficacy.

Overall, the results from this study indicate that hydrogen bonding, salt bridges, and hydrophobic interactions are key determinants of ligand binding affinity. The importance of these interactions in stabilizing the ligand-protein complex is consistent with previous studies that have emphasized the role of these forces in drug design (Lee et al., 2017). ZINC000026664090's superior binding affinity can be primarily attributed to its strong hydrogen bonding network and extensive hydrophobic interactions, making it the most promising lead compound. ZINC000019632917 and ZINC000060392785 also exhibited strong binding, albeit to a lesser extent, and warrant further optimization.

These findings not only improve our understanding of ligand-protein interactions but also provide a basis for future efforts in drug discovery and optimization. Future studies should focus on refining the structural features of these ligands to further enhance binding efficiency, selectivity, and overall therapeutic potential. Additionally, experimental validation through techniques such as X-ray crystallography or surface plasmon resonance would be valuable in confirming these computational predictions.

## Conclusion

The docking results revealed that ZINC000026664090 exhibited the highest binding affinity (-8 kcal/mol), followed by ZINC000019632917 (-7.4 kcal/mol) and ZINC000060392785 (-7.1 kcal/mol), suggesting that these ligands have strong potential for stable interactions with the target protein. The primary contributors to ligand stability were hydrogen bonding, electrostatic interactions (salt bridges and attractive charge interactions), and hydrophobic forces, including  $\pi$ - $\pi$  stacking and alkyl interactions. Notably, ZINC000026664090's superior affinity can be attributed to its strong hydrogen bonding network and extensive hydrophobic interactions, while ZINC000019632917 and ZINC000060392785 benefited from a combination of hydrogen bonds and electrostatic forces. The findings from this study provide valuable insights into ligand-protein interactions and can guide further optimization for improved binding efficiency and potential therapeutic applications.

## References

- Al-Zrkani, M. K., Abdulkareem, R. A., Al-Fahad, D., Al Shouber, M., Nasr, A. M. S., & Al-Khdhairawi, A. (2023). Elucidating novel antibacterial compounds from the NPASS database against the FimH lectin domain for the treatment of urinary tract infections: an in-silico study. *Journal of Biomolecular Structure and Dynamics*, 41(9), 3914-3925.
- Allocati, N., Masulli, M., Di Ilio, C., & Federici, L. (2018). Glutathione transferases: substrates, inhibitors and pro-drugs in cancer and neurodegenerative diseases. *Oncogenesis*, 7(1), 8.
- Andrianov, A. M., Nikolaev, G. I., Shuldov, N. A., Bosko, I. P., Anischenko, A. I., & Tuzikov, A. V. (2022). Application of deep learning and molecular modeling to identify small drug-like compounds as potential HIV-1 entry inhibitors. *Journal of Biomolecular Structure and Dynamics*, 40(16), 7555-7573.
- Bissantz, C., Kuhn, B., & Stahl, M. (2010). A medicinal chemist's guide to molecular interactions. *Journal of medicinal chemistry*, 53(14), 5061-5084.
- Chen, Y., Georgiou, T. T., & Pavon, M. (2021). Stochastic control liaisons: Richard sinkhorn meets gaspard monge on a schrodinger bridge. *Siam Review*, 63(2), 249-313.
- Hu, R.-S., Zhang, F.-K., Ma, Q.-N., Ehsan, M., Zhao, Q., & Zhu, X.-Q. (2022). Transcriptomic landscape of hepatic lymph nodes, peripheral blood lymphocytes and spleen of swamp buffaloes infected with the tropical liver fluke *Fasciola gigantica*. *PLoS Neglected Tropical Diseases*, 16(3), e0010286.
- Lalor, R., Cwiklinski, K., Calvani, N. E. D., Dorey, A., Hamon, S., Corrales, J. L., Dalton, J. P., & De Marco Verissimo, C. (2021). Pathogenicity and virulence of the liver flukes *Fasciola hepatica* and *Fasciola gigantica* that cause the zoonosis Fasciolosis. *Virulence*, 12(1), 2839-2867.
- Lee, J., Shi, Y., Vega, M., Yang, Y., Gera, J., Jung, M. E., & Lichtenstein, A. (2017). Structure-activity relationship study of small molecule inhibitors of the DEPTOR-mTOR interaction. *Bioorganic & Medicinal Chemistry Letters*, 27(20), 4714-4724.
- Li, F., & Liu, G. (2024). *Fasciola*. In *Molecular Medical Microbiology* (pp. 3249-3259). Elsevier.
- Nawar, A. M., Dawood, W. M., & Kadhem, N. Y. (2024). The effect of alcoholic extract of *Citrullus colocynthis* on the structural manifestations of the parasite *Fasciola gigantica* and its comparison with the drug pendazole. *Nabatia*, 12(1), 21-27.

- Shoulah, S. A., Gaballa, M. M., Al-Assas, M. M., Saqr, S. A., Gattan, H. S., & Selim, A. (2024). Histopathological changes and oxidative stress associated with Fascioliasis in bovines. *Tropical Animal Health and Production*, 56(2), 48.
- Su, W., Ai, Q., Li, X., Chen, J., Liu, Y., Wu, X., & Hou, S. (2024). Wikiformer: Pre-training with structured information of wikipedia for ad-hoc retrieval. *Proceedings of the AAAI Conference on Artificial Intelligence*,
- Trott, O., & Olson, A. J. (2010). AutoDock Vina: improving the speed and accuracy of docking with a new scoring function, efficient optimization, and multithreading. *Journal of computational chemistry*, 31(2), 455-461.
- Zhang, Y., Li, S., Meng, K., & Sun, S. (2024). Machine Learning for Sequence and Structure-Based Protein–Ligand Interaction Prediction. *Journal of chemical information and modeling*, 64(5), 1456-1472.
- Zhou, W., Yang, Y., Mei, C., Dong, P., Mu, S., Wu, H., Zhou, Y., Zheng, Y., Guo, F., & Yang, J.-Q. (2019). Inhibition of Rho-kinase downregulates Th17 cells and ameliorates hepatic fibrosis by *Schistosoma japonicum* infection. *Cells*, 8(10), 1262.